CRYSTAL GROWTH & DESIGN

Article

pubs.acs.org/crystal

Novel Bis(4,4′-dipyridylamine) Ligand with a Flexible Butadiyne Linker: Syntheses, Structures, and Photoluminescence of d^{10} Metal Coordination Polymers

Caixia Ding,[†] Xing Li,[‡] Yubin Ding,[†] Xin Li,[†] Seik Weng Ng,[§,#] and Yongshu Xie*,[†]

[†]Key Laboratory for Advanced Materials and Institute of Fine Chemicals, East China University of Science & Technology, Shanghai 200237, P. R. China

[‡]State Key Laboratory Base of Novel Functional Materials and Preparation Science, Faculty of Materials Science and Chemical Engineering, Ningbo University, Ningbo, Zhejiang 315211, P. R. China

[§]Department of Chemistry, University of Malaya, 50603, Kuala Lumpur, Malaysia

[#]Chemistry Department, Faculty of Science, King Abdulaziz University, PO Box 80203, Jeddah, Saudi Arabia

Supporting Information

ABSTRACT: The design and syntheses of novel ligands are essential for developing coordination compounds with novel structures and interesting properties. In this work, we designed and synthesized a novel ligand bis(4,4′-dipyridylaminophenylene)butadiyne (**L**) by attaching two 4,4′-dipyridylamine moieties to a flexible butadiyne linker. Starting from this novel ligand, seven coordination polymers $[Zn_2L(HCOO)_3(OH)]_n$ (**1**), $[Cd_2L_2Cl_4]_n\cdot 3n$DMF$\cdot 3nH_2O$ (**2**), $[CdLBr_2]_n$ (**3**), $[Cd_6L_3(SO_4)_6]_n\cdot 4n$MeCN (**4**), $[Hg_2LBr_4]_n\cdot 3nCH_2Cl_2\cdot nH_2O$ (**5**), $[Cu_2LI_2]_n\cdot 0.5nCH_2Cl_2$ (**6**), and $[Ag_2L(H_2O)_2]_n(NO_3)_{2n}\cdot 2nH_2O$ (**7**) were synthesized. Single-crystal X-ray diffraction analyses revealed that two forms of the ligand crystals, **L** and **L·0.5DMF** present straight and bent conformations, respectively, because of the flexibility of the butadiyne unit. A rich structural diversity was observed for its d^{10} metal complexes. Complexes **1** and **5** present ladder-like structures. In complexes **2** and **4**, the ligand molecules are linked by metal atoms to afford 3D supramolecular structures. It is noteworthy that the 3D structure of complex **4** consists of interesting infinite $\{Cd_6(SO_4)_6\}_\infty$ chains, whereas complexes **3**, **6**, and **7** exhibit 2D network structures. Interestingly, in the crystal of complex **7**, each ligand links four metal ions and each Ag ion bridges two ligands, leading to the formation of undulated 2D sheets with large cavities composed of 66-membered metallomacrocycles, which are interpenetrated by three other such 2D sheets, affording a 4-fold interpenetrated structure. In summary, the complex structures are dependent on the metal ions and the anions. In addition, the flexibility of the butadiyne moiety provides additional means for modulating the structures. Solid state photoluminescence of the free ligand and the complexes shows emission maxima within the range of 420−515 nm, which can be modulated by the conformations of the ligand in addition to the variation of the metal ions and anions, and the introduction of the butadiyne unit has a bathochromic effect.

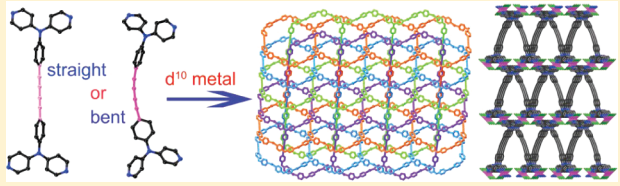

INTRODUCTION

The design and construction of coordination polymers containing metal ions and organic ligands have attracted much attention not only because of their intriguing variety of structures, but also for their potential applications in many fields.[1,2] It is well-known that inorganic−organic hybrid coordination polymers, especially those with d^{10} metal centers, exhibit photoluminescence and have potential applications as fluorescence-emitting materials, such as light-emitting diodes (LEDs).[3] Hence, the design and synthesis of coordination polymers containing d^{10} metal centers have received remarkable attention. One of the current interesting topics in this area is to rationally design organic ligands with efficient coordination groups and suitable conjugated systems. In this respect, both bridging and chelating pyridyl ligands have been intensely investigated due to the strong coordination ability and structural diversity. Thus, 2,2′-dipyridylamine (2,2′-dpa),[4] 4,4′-dipyridyl-amine (4,4′-dpa),[5] and their derivatives[6] have been proved to be efficient building blocks in the construction of coordination polymers with one-, two-, or three-dimensional structures.

During the past few years, our group has utilized 2,2′-dpa and 4,4′-dpa-derived ligands, including *N*,*N*-bis(2-pyridyl)-*N*′,*N*′-bis(4-pyridyl)-1,4-phenylenediamine (L^1, Scheme 1) and *N*,*N*,*N*′,*N*′-tetrakis(4-pyridyl)-1,4-phenylenediamine (L^2, Scheme 1), as building blocks in the construction of coordination polymers with tunable luminescent properties.[7] It can be expected that the design and utilization of similar tetrapyridyl ligands with various sizes of extended aromatic systems and various HOMO−LUMO gaps is a practical

Received: December 15, 2011
Revised: April 26, 2012
Published: May 23, 2012

Scheme 1. Structures of L^1, L^2, and L

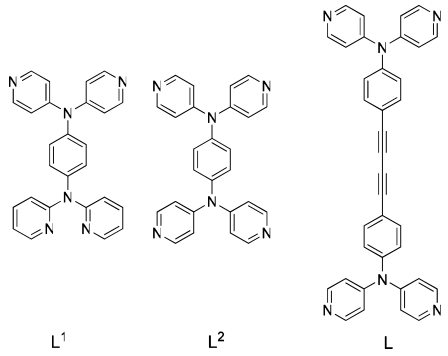

approach to further tuning the fluorescence wavelength and intensity of the coordination compounds. Thus, a novel butadiyne-containing tetrapyridyl ligand, bis(4,4′-dipyridylaminophenylene)butadiyne (**L**, Scheme 1) was designed. Compared with L^2, it offers some intriguing characteristics. First, the conjugated system is extended by the butadiyne moiety, which may be efficient to tune the fluorescence wavelength. Second, the ligand has better flexibility due to the bending and rotation of the butadiyne unit.[8] Thus, the conformational freedom may be better to satisfy the geometric needs of various metal ions in the construction of novel coordination polymers with diversified and intriguing architectures and topologies. On the basis of these considerations, in this work, we synthesized the novel ligand L, and utilized it for coordination with Zn(II), Cd(II), Hg(II), Cu(I), and Ag(I) to afford coordination polymers, $[Zn_2L(HCOO)_3(OH)]_n$ (**1**), $[Cd_2L_2Cl_4]_n \cdot 3n DMF \cdot 3n H_2O$ (**2**), $[CdLBr_2]_n$ (**3**), $[Cd_6L_3(SO_4)_6]_n \cdot 4n MeCN$ (**4**), $[Hg_2LBr_4]_n \cdot 3n CH_2Cl_2 \cdot n H_2O$ (**5**), $[Cu_2LI_2]_n \cdot 0.5n CH_2Cl_2$ (**6**), and $[Ag_2L(H_2O)_2]_n(NO_3)_{2n} \cdot 2n H_2O$ (**7**).

These complexes exhibit a rich structural diversity, including ladder-like structures, 2D networks containing (Cu_2I_2) units, 3D structures consisting of infinite $\{Cd_6(SO_4)_6\}_\infty$ chains, and a 4-fold interpenetrated 2D structure. In addition, it is noteworthy that two different crystals of the ligand, namely, **L** and **L·0.5 DMF** were obtained from MeOH and DMF, respectively, and they contain the butadiyne moieties in the straight and bent conformations, respectively. Both conformations are also observed in the complexes. The solid state emission maxima of these compounds lie in the range between 420 and 515 nm, and the emission behavior can be well tuned.

EXPERIMENTAL SECTION

Materials. All chemicals of reagent grade quality were used as received from commercial sources. (4-Bromophenyl)- di(4-pyridyl)-amine was prepared as we previously reported.[7a]

Physical Measurements. ^{1}H NMR spectra were recorded on a Bruker AVANCE spectrometer (400 MHz). FT-IR spectra were recorded in the region of 400−4000 cm^{-1} on a Thermo Electron Avatar 380 FT-IR instrument (KBr Discs). Elemental analyses were carried out with an Elmentar Vario EL-III analyzer. Fluorescence measurements were performed on a Varian Cary Eclipse fluorescence spectrophotometer. HRMS were performed using a Waters LCT Premier XE spectrometer.

Synthesis and Crystal Growth. Bis(4,4′-dipyridylaminophenylene)butadiyne (**L**) (4-bromo-phenyl)-di(4-pyridyl)amine (6.52 g, 20 mmol), tetrakis(tri- phenylphosphine) palladium (1.16 g, 1.0 mmol), cuprous iodide (400 mg, 2.1 mmol), trimethylsilylacetylene (TMSA) (7.1 mL, 50 mmol), diisopropylamine (33.4 mL, 237 mmol), and *N*,*N*-Dimethylformamide (270 mL) were added to a three-necked flask (500 mL) and heated at 130 °C under N_2 for 4 days. After the reaction was cooled, the majority of DMF was removed by rotary evaporation. The residue was purified by a silica gel column to afford a colorless solid of the ligand **L** (590 mg, yield 11%). Crystals of **L** were obtained by the slow evaporation of a MeOH solution of **L** for a few days at room temperature, and the crystals of **L·0.5DMF** were obtained by heating a solution of L (10 mg, 0.02 mmol) in DMF (1 mL) and H_2O (0.5 mL) at 120 °C, followed by cooling to room temperature. ^{1}H NMR ($CDCl_3$, 400 MHz): δ = 8.46 (d, J = 6.0 Hz, 8H, pyridyl-H), 7.56 (d, J = 8.4 Hz, 4H, phenylene-H), 7.15 (d, J = 8.8 Hz, 4H, phenylene-H), 6.97 (m, 8H, pyridyl-H). Anal. Calcd (%) for $C_{36}H_{24}N_6$: C, 79.98; H, 4.47; N, 15.55. Found: C, 79.90; H, 4.34; N, 15.62. IR (KBr pellet, cm^{-1}): 3441(br), 3017(w), 2921(w), 2847(w), 1578(vs), 1492(s), 1402(w), 1386(w), 1338(m), 1300(m), 1281(m), 1214(m),1175(w), 989(m), 935(w), 810(m), 733(w), 695(w), 618(m), 557(w), 538(w). HRMS: obsd 541.2142, calcd for $C_{36}H_{25}N_6$ ($[M + H]^+$): 541.2141.

Scheme 2. Preparation of Ligand L

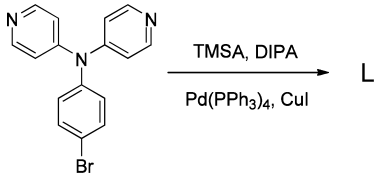

*$[Zn_2L(HCOO)_3(OH)]_n$ (**1**).* A mixture of **L** (5.4 mg, 0.01 mmol), $Zn(ClO_4)_2 \cdot 6H_2O$ (7.4 mg, 0.02 mmol), and $HCOONa \cdot 2H_2O$ (4.2 mg, 0.04 mmol) in DMF, MeCN and H_2O (8: 12: 1) was sealed in a 10 mL Teflon lined stainless steel vessel under autogenous pressure and heated to 150 °C for 100 h. After cooling to room temperature, yellowish crystals of **1** suitable for X-ray structure determination were obtained. Yield: 4 mg, 52%. Anal. (%) Calcd for $C_{39}H_{28}N_6O_7Zn_2$: C, 56.88; H, 3.43; N, 10.21. Found: C, 57.12; H, 3.35; N, 10.37. IR (KBr pellet, cm^{-1}): 3420(br), 2917(w), 2844(w), 1619(s), 1598(vs), 1497(s), 1383(m), 1347(m), 1313(m), 1217(m), 1066(m), 1025(s), 992(m), 826(m), 739(w), 634(m), 538(m).

*$[Cd_2L_2Cl_4]_n \cdot 3n DMF \cdot 3n H_2O$ (**2**).* A mixture of **L** (5.4 mg, 0.01 mmol), $Cd(NO_3)_2 \cdot 4H_2O$ (6.2 mg, 0.02 mmol), and NaCl (2.2 mg, 0.04 mmol) in DMSO, DMF, and H_2O (12: 9: 0.5) was sealed in a small vial (10 mL), which was heated to 120 °C for 120 h. After it was cooled to room temperature, colorless block crystals of **2** were obtained. Yield: 4 mg, 54%. Anal. (%) Calcd for $C_{81}H_{75}Cd_2Cl_4N_{15}O_6$: C, 56.52; H, 4.39; N, 12.21. Found: C, 56.73; H, 4.28; N, 12.38. IR (KBr pellet, cm^{-1}): 3442(br), 2926(w), 2851(w), 1615(m), 1582(vs), 1496(vs), 1383(m), 1341(m), 1308(m), 1283(m), 1217(m), 1064(m), 1013(s), 992(s), 819(m), 736(w), 694(w), 624(m), 541(m).

*$[CdLBr_2]_n$ (**3**).* Compound **3** was prepared by a procedure similar to that for **2**, using KBr (4.8 mg, 0.04 mmol) in place of NaCl. Colorless block crystals of **3** were obtained. Yield: 5 mg, 63%. Anal. (%) Calcd for $C_{36}H_{24}Br_2CdN_6$: C, 53.19; H, 2.98; N, 10.34. Found: C, 53.23; H, 2.92; N,10.42. IR (KBr pellet, cm^{-1}): 3418(br), 2920(w), 2851(w), 1636(m), 1617(m), 1591(s), 1496(s), 1385(w), 1344(m), 1314(w), 1294(m), 1216(m), 1061(m), 1013(s), 827(w), 742(w), 627(m), 565(m), 541(m), 469(m).

*$[Cd_6L_3(SO_4)_6]_n \cdot 4n MeCN$ (**4**).* Compound **4** was prepared by a procedure similar to that for **2** from the reaction of **L** (5.4 mg, 0.01 mmol) and $CdSO_4$ (2 mg, 0.02 mmol) in DMF, MeCN, and H_2O (5: 10: 1). Yellowish crystals of **4** were obtained. Yield: 5 mg, 49%. Anal. (%) Calcd for $C_{116}H_{84}Cd_6N_{22}O_{24}S_6$: C, 45.88; H, 2.79; N, 10.15. Found: C, 45.62; H, 2.71; N, 10.03. IR (KBr pellet, cm^{-1}): 3433(br), 2919(w), 2847(w), 1637(m), 1613(m), 1588(s), 1495(s), 1400(s), 1384(vs), 1316(w), 1281(w), 1217(w), 1146(vs), 986(m), 941(w), 816(w), 621(m), 493(m), 467(m).

*$[Hg_2LBr_4]_n \cdot 3n CH_2Cl_2 \cdot n H_2O$ (**5**).* A solution of $Hg(NO_3)_2$ (6 mg, 0.016 mmol) and KBr (4 mg, 0.032 mmol) in methanol (3 mL) was layered over a solution of **L** (4.2 mg, 0.008 mmol) in CH_2Cl_2(3 mL).

dx.doi.org/10.1021/cg201655n | *Cryst. Growth Des.* 2012, 12, 3465−3473

Table 1. Crystallographic Data and Structure Refinements Summary for L, L·0.5DMF, and the Metal Complexes

	L	L·0.5DMF	2	3	4	5	6	7
empirical formula	$C_{36}H_{24}N_6$	$C_{39}H_{31}N_7O$	$C_{81}H_{75}Cd_2Cl_4N_{15}O_6$	$C_{36}H_{24}Br_2CdN_6$	$C_{116}H_{84}Cd_6N_{22}O_{24}S_6$	$C_{19.50}H_{16}Br_2Cl_3HgN_3O_{0.50}$	$C_{36.50}H_{25}ClCu_2I_2N_6$	$C_{18}H_{16}AgN_4O_5$
fw	540.61	613.71	1721.16	812.83	3036.81	767.11	963.96	476.22
crystal system	monoclinic	triclinic	monoclinic	monoclinic	triclinic	monoclinic	triclinic	monoclinic
space group	$P2_1/c$	$P\bar{1}$	$P2_1/c$	$P2/n$	$P\bar{1}$	$C2/c$	$P\bar{1}$	$P2/n$
T (K)	298(2)	293(2)	298(2)	298(2)	298(2)	100(2)	298(2)	298(2)
a (Å)	11.6529(11)	8.8313(5)	20.613(2)	7.7348(7)	10.1093(12)	19.6356(9	8.4628(12)	13.0282(13)
b (Å)	7.8862(8)	9.8210(6)	12.7980(11)	10.3163(11)	13.0570(13)	16.0764(8)	10.6640(15)	9.5994(8)
c (Å)	16.1128(18)	20.9307(13)	18.8901(17)	24.542(2)	24.3590(19)	30.783(3)	11.8808(19)	17.9846(17)
α (deg)	90	78.3320(10)	90	90	85.542(2)	90	80.5110(10)	90
β (deg)	98.7540(10)	81.6130(10)	104.4500(10)	90.3530(10)	85.314(2)	101.453(6)	70.4030(10)	90.2160(10)
γ (deg)	90	67.0860(10)	90	90	80.7490(10)	90	86.894(2)	90
V (Å^3)	1463.5(3)	1633.02(17)	4825.6(8)	1958.2(3)	3156.1(5)	9523.8(11)	996.3(3)	2249.2(4)
Z	2	2	2	2	1	16	1	4
D_{calcd} (Mg/m^3)	1.227	1.248	1.185	1.379	1.598	2.140	1.607	1.406
μ (mm^{-1})	0.075	0.078	0.603	2.628	1.168	10.171	2.715	0.928
no. of reflns ($I > 2\sigma(I)$)	2577	5687	8493	3426	10968	10529	3469	3482
Final R_1[a] [$I > 2\sigma(I)$]	0.0488	0.0530	0.0761	0.0731	0.0525	0.0866	0.0651	0.0776
R_2[b] (all data)	0.0948	0.1677	0.2387	0.1635	0.1279	0.2762	0.1597	0.2344
goodness of fit	1.028	1.041	1.035	1.045	1.041	1.094	1.083	0.883

[a] $R_1 = \Sigma||F_o| - |F_c||/\Sigma|F_o|$. [b] $R_2 = \Sigma||F_o| - |F_c||w^{1/2}/\Sigma|F_o|w^{1/2}$.

Yellowish single crystals of **5** were obtained by slow interlayer diffusion for several weeks. Yield: 3 mg, 47%. Anal. (%) Calcd for $C_{19.50}H_{16}Br_2Cl_3HgN_3O_{0.50}$: C, 30.53; H, 2.10; N, 5.48. Found: C, 30.70; H, 2.04; N, 5.62. IR (KBr pellet, cm^{-1}): 3413(br), 2974(m), 2896(w), 1638(w), 1616(w), 1590(vs), 1499(s), 1384(m), 1340(s), 1302(m), 1287(w), 1217(w), 1088(m), 1049(s), 1012(m), 937(w), 880(m), 819(w), 737(w), 647(m), 541(w), 495(w).

*$[Cu_2LI_2]_n$·0.5nCH_2Cl_2 (**6**).* Compound **6** was prepared by a procedure similar to that for **5**, using a solution of CuI (3 mg, 0.016 mmol) in MeCN in place of a methanol solution of $Hg(NO_3)_2$ and KBr. Single crystals of **6** were obtained by slow interlayer diffusion for several weeks. Yield: 4 mg, 55%. Anal. (%) Calcd for $C_{36.50}H_{25}ClCu_2I_2N_6$: C, 45.48; H, 2.61; N, 8.72. Found: C, 45.73; H, 2.68; N, 8.85. IR (KBr pellet, cm^{-1}): 3415(br), 2917(m), 2847(w), 1637(m), 1617(s), 1590(s), 1559(w), 1489(s), 1400(w), 1384(s), 1337(w), 1285(w), 1212(m), 1014(w), 820(w), 736(w), 627(m), 476(m).

*$[Ag_2L(H_2O)_2]_n(NO_3)_{2n}$·2n$H_2O$ (**7**).* A solution of **L** (4.2 mg, 0.008 mmol) in methanol (3 mL) was layered over a solution of $AgNO_3$ (6 mg, 0.016 mmol) in H_2O (3 mL). Single crystals of **7** were obtained by slow interlayer diffusion for several weeks. Yield: 5 mg, 66%. Anal. (%) Calcd for $C_{18}H_{16}AgN_4O_{4.5}$: C, 46.17; H, 3.44; N, 11.97. Found: C, 46.42; H, 3.36; N, 12.08. IR (KBr pellet, cm^{-1}): 3447(br), 2920(m), 2847(w), 1614(m), 1589(s), 1492(s), 1384(vs), 1342(m), 1309(m), 1287(w), 1219(w), 1146(w), 993(m), 938(w), 820(m), 723(w), 618(m).

X-ray Crystallography. X-ray diffraction data were collected on a Bruker-AXS APEX diffractometer utilizing MoKα radiation (λ = 0.71073 Å). The structures were solved by direct methods and refined with full-matrix least-squares technique. Anisotropic thermal parameters were applied to all non hydrogen atoms. All of the hydrogen atoms in these structures are located from the differential electron density map and constrained to the ideal positions in the refinement procedure. All calculations were performed using SHELX-97 software package.[9] Crystal data and experimental details for the crystals are summarized in Table 1 and S1, and selected bond lengths and bond angles are given in Table 2 and S2.

DFT Calculations. The calculations were carried out by using the Gaussian03 program package.[10] The geometries of L^2 and L were optimized by density functional calculations employing the hybrid B3LYP function.[11] The 6-31G* basis set[12] was adopted to describe all atoms. The calculated HOMO/LUMO energies are listed in Table S3. Molecular structures and molecular orbitals were visualized by the Gabedit software.[13]

RESULTS AND DISCUSSION

Synthesis and Characterization. The ligand **L** was prepared from a one-pot synthesis comprising of a Sonogashira coupling reaction of (4-bromophenyl)-bis(4-pyridyl)amine with trimethylsilylacetylene (TMSA) in DMF followed by an oxidative dimerization, using tetrakis(triphenyl-phosphine)-palladium, cuprous iodide, and diisopropylamine as catalysts and the base, respectively. When the reaction was performed at 80 °C, no reaction could be detected by TLC, so we tried to increase the reaction temperature. Thus the reaction was performed at 130 °C for 4 days to afford L. At first, in the reaction, the single-ethyne product was formed, then the alkynyl group is successively transferred from silicon to copper to generate alkynylcopper species, which then oxidatively dimerize to furnish the diacetylene compound L.[14] It is noteworthy that two forms of ligand crystals were obtained by two different methods: the form of L was obtained by slow evaporation of the MeOH solution at room temperature, and the form of L·0.5DMF was obtained by heating the ligand in a mixed solvent of DMF and H_2O followed by cooling to room temperature. Single crystals of complexes **1**−**4** were obtained by solvothermal reactions of the corresponding metal salts with the ligand L and the crystals of complexes **5**−**7** were obtained by slow interlayer diffusion between the solutions of the ligand and corresponding metal salts. Thus, the two different ligand

dx.doi.org/10.1021/cg201655n | Cryst. Growth Des. 2012, 12, 3465−3473

Table 2. Selected Bond Lengths (Å) and Angles (deg) for the Metal Complexes 2−7

complex **2**							
Cd(1)−N(2)	2.364(7)	N(2)−Cd(1)−N(6)	179.5(3)	N(2)−Cd(1)−Cl(2)	90.1(2)	N(6)−Cd(1)−Cl(1)	91.1(2)
Cd(1)−N(6)	2.382(7)	N(2)−Cd(1)−N(5)	92.3(3)	N(6)−Cd(1)−Cl(2)	90.0(2)	N(5)−Cd(1)−Cl(1)	89.4(2)
Cd(1)−N(5)	2.393(8)	N(6)−Cd(1)−N(5)	87.3(3)	N(5)−Cd(1)−Cl(2)	93.1(2)	N(3)−Cd(1)−Cl(1)	88.8(2)
Cd(1)−N(3)	2.400(8)	N(2)−Cd(1)−N(3)	90.3(3)	N(3)−Cd(1)−Cl(2)	88.7(2)	Cl(2)−Cd(1)−Cl(1)	177.26(9)
Cd(1)−Cl(2)	2.600(3)	N(6)−Cd(1)−N(3)	90.1(3)	N(2)−Cd(1)−Cl(1)	88.7(2)		
Cd(1)−Cl(1)	2.630(3)	N(5)−Cd(1)−N(3)	176.8(2)				
complex **3**[a]							
Cd(1)−N(3)#1	2.382(8)	N(3)#1−Cd(1)−N(3)#2	92.7(4)	N(3)#1−Cd(1)−Br(1)#3	88.3(2)	N(2)−Cd(1)−Br(1)	92.1(3)
Cd(1)−N(3)#2	2.382(8)	N(3)#1−Cd(1)−N(2)	174.5(4)	N(3)#2−Cd(1)−Br(1)#3	92.4(2)	N(2)#3−Cd(1)−Br(1)	87.1(3)
Cd(1)−N(2)	2.400(8)	N(3)#2−Cd(1)−N(2)	90.5(3)	N(2)−Cd(1)−Br(1)#3	87.1(3)	Br(1)#3−Cd(1)−Br(1)	178.96(9)
Cd(1)−N(2)#3	2.400(8)	N(3)#1−Cd(1)−N(2)#3	90.5(3)	N(2)#3−Cd(1)−Br(1)#	92.1(3)		
Cd(1)−Br(1)#3	2.7470(14)	N(3)#2−Cd(1)−N(2)#3	174.5(4)	N(3)#1−Cd(1)−Br(1)	92.4(2)		
Cd(1)−Br(1)	2.7470(14)	N(2)−Cd(1)−N(2)#3	86.7(4)	N(3)#2−Cd(1)−Br(1)	88.3(2)		
complex **4**[b]							
Cd(1)−O(5)	2.263(5)	Cd(3)−O(3)#2	2.350(5)	O(9)−Cd(2)−N(3)	96.6(2)	N(6)#3−Cd(3)−O(7)#2	77.14(19)
Cd(1)−O(12)#1	2.271(5)	Cd(3)−O(6)#2	2.448(5)	O(8)#2−Cd(2)−O(6)	102.30(18)	N(8)−Cd(3)−O(7)#2	163.7(2)
Cd(1)−N(5)	2.295(6)	Cd(3)−O(7)#2	2.530(6)	O(10)−Cd(3)−O(7)#2	111.98(19)	O(9)−Cd(2)−O(6)	83.82(17)
Cd(1)−O(1)	2.329(4)	O(5)−Cd(1)−N(2)	86.74(18)	O(3)#2−Cd(3)−O(7)#2	89.65(18)	N(3)−Cd(2)−O(6)	167.30(18)
Cd(1)−N(2)	2.345(5)	O(12)#1−Cd(1)−N(2)	88.22(19)	O(6)#2−Cd(3)−O(7)#2	56.25(16)	O(8)#2−Cd(2)−O(2)	104.71(17)
Cd(1)−O(9)	2.441(4)	N(5)−Cd(1)−N(2)	108.7(2)	N(6)#3−Cd(3)−O(10)	138.6(2)	O(9)−Cd(2)−O(2)	133.67(16)
Cd(2)−O(8)#2	2.185(5)	O(1)−Cd(1)−N(2)	87.17(18)	N(8)−Cd(3)−O(10)	83.0(2)	N(3)−Cd(2)−O(2)	89.21(19)
Cd(2)−O(9)	2.248(4)	O(5)−Cd(1)−O(9)	80.65(17)	N(6)#3−Cd(3)−O(3)#2	88.78(19)	O(6)−Cd(2)−O(2)	81.49(17)
Cd(2)−N(3)	2.302(6)	O(12)#1−Cd(1)−O(9)	106.10(16)	N(8)−Cd(3)−O(3)#2	85.0(2)	O(8)#2−Cd(2)−O(1)	161.97(16)
Cd(2)−O(6)	2.313(5)	N(5)−Cd(1)−O(9)	84.44(18)	O(10)−Cd(3)−O(3)#2	129.9(2)	O(9)−Cd(2)−O(1)	76.67(15)
Cd(2)−O(2)	2.331(4)	O(1)−Cd(1)−O(9)	78.28(15)	N(6)#3−Cd(3)−O(6)#2	132.45(18)	N(3)−Cd(2)−O(1)	88.14(17)
Cd(2)−O(1)	2.590(5)	N(2)−Cd(1)−O(9)	159.51(18)	N(8)−Cd(3)−O(6)#2	137.7(2)	O(6)−Cd(2)−O(1)	79.58(15)
Cd(3)−N(6)#3	2.282(6)	O(8)#2−Cd(2)−O(9)	121.32(17)	O(10)−Cd(3)−O(6)#2	74.73(18)	O(2)−Cd(2)−O(1)	57.56(15)
Cd(3)−N(8)	2.345(6)	O(8)#2−Cd(2)−N(3)	88.4(2)	O(3)#2−Cd(3)−O(6)#2	82.58(16)	N(6)#3−Cd(3)−N(8)	87.3(2)
Cd(3)−O(10)	2.348(6)						
complex **5**[c]							
Hg(1)−N(1)	2.386(13)	Hg(2)−Br(3)	2.510(2)	N(6)#1−Hg(1)−Br(1)	100.4(3)	N(4)#2−Hg(2)−Br(3)	107.1(4)
Hg(1)−N(6)#1	2.416(14)	Hg(2)−Br(4)	2.517(2)	N(1)−Hg(1)−Br(2)	100.2(3)	N(3)−Hg(2)−Br(3)	102.6(4)
Hg(1)−Br(1)	2.492(2)	N(4)−Hg(2)#2	2.340(15)	N(6)#1−Hg(1)−Br(2)	99.4(3)	N(4)#2−Hg(2)−Br(4)	98.8(4)
Hg(1)−Br(2)	2.500(2)	N(6)−Hg(1)#1	2.416(14)	Br(1)−Hg(1)−Br(2)	149.80(7)	N(3)−Hg(2)−Br(4)	99.6(3)
Hg(2)−N(4)#2	2.340(15)	N(1)−Hg(1)−N(6)#1	89.7(4)	N(4)#2−Hg(2)−N(3)	103.3(5)	Br(3)−Hg(2)−Br(4)	140.60(7)
Hg(2)−N(3)	2.350(13)	N(1)−Hg(1)−Br(1)	102.5(3)				
complex **6**[d]							
Cu(1)−N(3)#1	2.040(7)	Cu(1)−I(1)	2.7139(18)	N(2)−Cu(1)−I(1)#2	108.8(2)	N(3)#1−Cu(1)−I(1)	103.6(2)
Cu(1)−N(2)	2.066(7)	I(1)−Cu(1)#2	2.6273(15)	N(3)#1−Cu(1)−Cu(1)#2	128.3(2)	N(2)−Cu(1)−I(1)	100.1(3)
Cu(1)−I(1)#2	2.6273(15)	N(3)#1−Cu(1)−N(2)	110.6(3)	N(2)−Cu(1)−Cu(1)#2	119.9(2)	I(1)#2−Cu(1)−I(1)	120.61(5)
		N(3)#1−Cu(1)−I(1)#2	112.3(2)	I(1)#2−Cu(1)−Cu(1)#2	61.94(5)	Cu(1)#2−I(1)−Cu(1)	59.39(5)
complex **7**[e]							
Ag(1)−N(3)	2.139(7)	Ag(1)−O(1)	2.687(14)	N(2)−Ag(1)−O(1)	96.7(4)	N(3)−Ag(1)−O(1)	103.4(4)
Ag(1)−N(2)	2.156(6)	N(3)−Ag(1)−N(2)	159.3(3)				

[a]Symmetry transformations used to generate equivalent atoms: #1 $-x + 5/2, y + 1, -z + 1/2$; #2 $x, y + 1, z$ #3 $-x + 5/2, y, -z + 1/2$; #4 $x, y - 1, z$; #5 $-x, -y, -z + 1$. [b]Symmetry transformations used to generate equivalent atoms: #1 $-x + 1, -y + 1, -z + 1$; #2 $-x + 2, -y + 1, -z + 1$; #3 $-x + 1, -y + 2, -z + 1$; #4 $x, y - 1, z$; #5 $-x + 2, -y, -z + 1$; #6 $-x + 1, -y, -z$; #7 $x, y + 1, z$; #8 $x - 1, y, z - 1$; #9 $x + 1, y, z + 1$. [c]Symmetry transformations used to generate equivalent atoms: #1 $-x + 3/2, -y + 5/2, -z + 1$; #2 $-x + 5/2, -y + 5/2, -z + 1$. [d]Symmetry transformations used to generate equivalent atoms: #1 $x, y - 1, z$; #2 $-x + 2, -y, -z + 1$; #3 $-x, -y + 2, -z + 2$; #4 $x, y + 1, z$; #5 $-x - 1, -y + 1, -z + 2$. [e]Symmetry transformations used to generate equivalent atoms:#1 $x + 1/2, -y + 1, z + 1/2$; #2 $-x + 1/2, y, -z + 3/2$; #3 $-x + 1/2, y, -z + 1/2$; #4 $-x + 1, -y - 1, -z + 2$; #5 $x - 1/2, -y + 1, z - 1/2$.

crystals and complexes **1**−**7** were characterized by single-crystal X-ray diffraction analyses.

Crystal Structures of L and L·0.5DMF. The molecule of ligand L in the crystal obtained from MeOH is centrosymmetric (Figure 1a). The butadiyne unit and the phenylene moieties are coplanar, and the dpa moieties are deviated from a planar structure due to steric hindrance. The dihedral angle between the neighboring pyridyl rings is 54.1(1)°, and the angles between the phenylene and the pyridyl rings are 70.0(8) and 70.3(5)°, respectively. The butadiyne unit of L adopts an approximately straight line conformation.

In the crystal of L·0.5 DMF, the butadiyne unit and the two phenylene moieties are nonplanar (Figure 1b), which is in sharp contrast to the planar structure observed in the crystal of L obtained from MeOH. The two phenylene rings are approximately vertical, with the dihedral angle of 90.4(1)°.

dx.doi.org/10.1021/cg201655n | Cryst. Growth Des. 2012, 12, 3465−3473

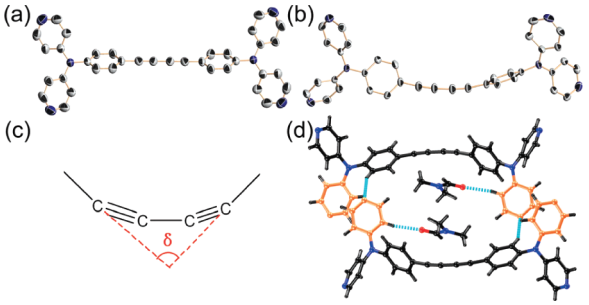

Figure 1. Molecular structures with thermal ellipsoids at the 50% probability level for L (a) and L·0.5DMF (b). Hydrogen atoms and DMF molecules are omitted for clarity. (c) The figure showing the angle δ for describing the bending of the butadiyne unit. (d) An $[L(DMF)]_2$ dimeric unit in the crystal of L·0.5DMF formed by intermolecular hydrogen bonds and $\pi\cdots\pi$ interactions.

And the butadiyne unit adopt a bent conformation. The bending can be described by the angle δ between the single bonds attached to the butadiyne unit (Figure 1c). Thus, for a straight conformation, the δ value is 180°, and for bent conformations, δ will be smaller than 180°. The δ value in the crystal of L·0.5 DMF was found to be 155.4(3)°, indicating a severe distortion of the butadiyne unit, which may result in a decrease in the π conjugation system and a blue shift of the emission peaks (vide infra). Interestingly, hydrogen bonds are observed between the pyridyl N atoms of the 4,4′-dpa moieties and the phenylene H atoms of neighboring ligand molecules, with the H···N distances of 2.51 Å, and the C−H···N angles of 153°. In addition, slipped parallel $\pi\cdots\pi$ stacking interactions between the pyridyl rings are observed, with the interplane angles of 23.2(4)°, and the centroid···centroid distances of 4.58 Å. These values lie above the optimal distance for $\pi\cdots\pi$ stacking.[15] Thus, the two ligand molecules are linked to afford a dimeric structure. It is noteworthy that the dimer is also involved in intermolecular hydrogen bonds with two DMF molecules, with the H···O distances of 2.40 Å and the C−H···O angles of 166°, thus a $[L\ (DMF)]_2$ dimer is formed. Hence, the wide occurrence of intermolecular hydrogen bonds and $\pi\cdots\pi$ interactions may account for the severe distortion of the butadiyne unit.

The presence of different conformations of L may provide an efficient approach for the construction of diversified and intriguing coordination architectures and topologies, which is demonstrated by the following crystal structures.

Crystal Structure of $[Zn_2L(HCOO)_3(OH)]_n$ (1). The crystal data quality for complex **1** is relatively poor with an R1 value of 0.1198, which cannot be significantly lowered even after repeated crystal growth and X-ray diffraction measurements. It shows a rough ladder-like structure (Supporting Information Figure S3). Related data are summarized in Supporting Information Table S1 and S2.

Crystal Structure of $[Cd_2L_2Cl_4]_n\cdot 3n DMF\cdot 3nH_2O$ (2). Crystal structure of compound **2** is shown in Figure 2. L utilizes all its pyridyl nitrogens to coordinate with four Cd(II) atoms. Each Cd(II) has a distorted octahedral coordination geometry, with four pyridyl nitrogens coordinated in the equatorial plane and two chlorides coordinated at the axial positions, which is different from the tetrahedral coordination geometry of Zn(II) observed in complex **1**. The L ligands adopt embowed conformations with the δ value of 168.3(1)°, and the Cd−N and Cd−Cl bond lengths lie in the ranges of 2.364(7)−

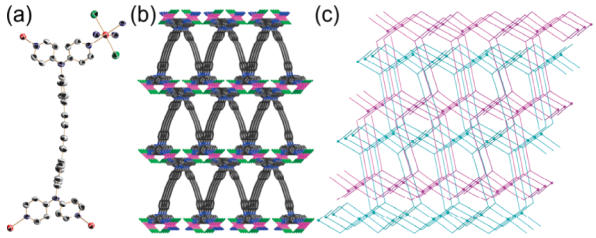

Figure 2. (a) View showing coordination environments of the Cd(II) centers in complex **2** with thermal ellipsoids at the 50% probability level. DMF and water have been omitted for clarity. (b) A 3D coordination network of complex **2**. (c) Topological view of **2**.

2.400(8) Å, and 2.600(3)−2.630(3) Å, respectively. These values lie within the normal range for Cd−N and Cd−Cl lengths in similar complexes.[7,16] Each Cd(II) links four ligands and each ligand links four Cd(II), which can be simplified as four−connected nodes, thus, affording a well-known uninodal **cds** net, which is interpenetrated by another such **cds** net, affording a 2-fold interpenetrated structure. Alternatively, the central N atoms of dpa units and the Cd(II) ions can be considered as 3- and 4-connected nodes, respectively, thus, the structure of **2** is a three-dimensional 2-fold interpenetrated network with the Schläfli symbol of $\{8^3\}_2\{8^5;10\}$, which was obtained by *TOPOS4*[17](Figure 2c).

Crystal Structure of $[CdLBr_2]_n$ (3). In the crystal structure of complex **3** (Figure 3), the coordination environment of each

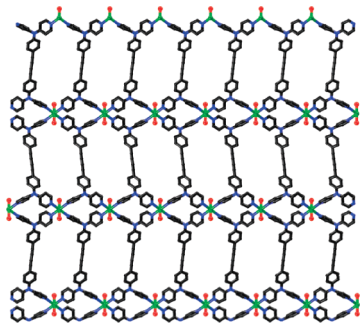

Figure 3. 2D coordination network of **3**.

Cd(II) is octahedral, which is similar to that observed in complex **2**, except the coordination of bromine in place of chlorine atoms. Cd−N distances are 2.382(8) and 2.400(8) Å, similar to those observed in complex **2**. Cd−Br distance is 2.7470(14) Å, which is within the typical Cd−Br bond length range as previously reported.[18] The ligand L adopts an approximately straight conformation, and the ligand molecules are linked by Cd atoms to form 46- and 20-membered metallomacrocycles, with the closest Cd···Cd distances of 22.98 and 10.32 Å, respectively. These metallomacrocycles are interconnected to afford a 2-D network. The structural difference between **2** and **3** may be caused by the difference in the anions, and it may also be ascribed to the difference in the conformations of the ligands. Both Cd(II) atoms and ligands are four−connected. Thus, the topology of **3** can be described as a uninodal 4^4-**sql** net. Alternatively, the central N atoms of dpa units can be considered as three-connected nodes and Cd(II) can be treated as four-connected nodes. On the basis of this simplification, the topology of 3 is a (3,4)-connected two-dimensional network with the Schläfli symbol of $\{4;\ 6^2\}_2\{4^2;\ 6^2;\ 8^2\}$ (Supporting Information Figure S4).

dx.doi.org/10.1021/cg201655n | *Cryst. Growth Des.* 2012, 12, 3465−3473

Crystal Structure of $[Cd_6L_3(SO_4)_6]_n \cdot 4n$MeCN (4). Complex **4** was obtained from the reaction of L and $CdSO_4$ in CH_3CN and DMF. It has an interesting $Cd_6(SO_4)_6$ core structure (Figure 4a) which consists of three different types of

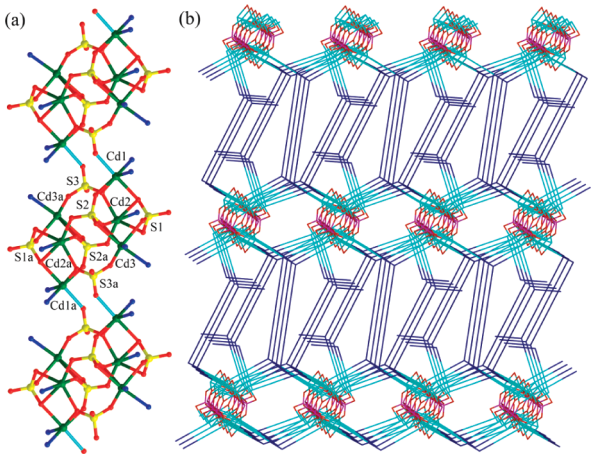

Figure 4. (a) $\{Cd_6(SO_4)_6\}_\infty$ chains in complex **4**. Symmetry operations: (a) $-x + 1, -y + 1, -z + 1$; (b) $-x + 2, -y + 1, -z + 1$. (b) Topological view of **4**.

crystallographically independent Cd(II) atoms. Cd1, Cd2, and Cd3 atoms have similar distorted octahedral coordination geometries. Cd1 coordinates with two pyridyl nitrogens from two L ligands and four O atoms from four sulfate anions, Cd2 is ligated by five O atoms from four different sulfate anions and one pyridyl nitrogen from L, and Cd3 is coordinated by two pyridyl nitrogens from two L ligands, two O atoms from two sulfate anions and two O atoms from one chelating sulfate anion. The Cd−N distances for the pyridyl groups and the Cd−O distances for sulfate anions lie in the ranges of 2.282(6)−2.345(5) Å and 2.185(5)−2.590(5)Å, respectively. One of the interesting structural aspects of this compound is the rich coordination modes of the sulfates, including two tridentate sulfates (S1 and S3) and one tetradentate sulfate (S2), which binds four Cd atoms within one Cd_6 unit. The average S−O distance of 1.434 Å for the noncoordinated oxygens are shorter than that of 1.471 Å for the coordinated oxygens, which is consistent with previous observations.[19] The tridentate sulfate of S3 bridges two neighboring $Cd_6(SO_4)_6$ cores, thus affording infinite $\{Cd_6(SO_4)_6\}_\infty$ chains, which are further bridged by the L ligands to form a 3D coordination framework (Figure 4b). To the best of our knowledge, it is the first example of a complex incorporating hexanuclear $Cd_6(SO_4)_6$ clusters as building blocks to form a 3D network structure. Topologically, the ligands can be treated as 3- and 4-connectors, and the complex structure can be simplified by TOPOS4[17] using cluster representation, resulting in a new 8,9,12 -connected topological net with the Schläfli symbol of $\{3^{10};4^{14};5^4\}\{3^{14};4^{14};5^8\}\{3^{15};4^{24};5^{26};6\}$.

Crystal Structure of $[Hg_2LBr_4]_n \cdot 3n CH_2Cl_2 \cdot nH_2O$ (5). The asymmetric unit of crystal **5** (Figure 5) consists of two crystallographically independent Hg(II) atoms and each Hg(II) atom locates in a distorted tetrahedral coordination environment, provided by two bromides and two pyridyl nitrogen atoms. The ligands show embowed conformations with the δ value of 168.0(1)°. Hg2−N distances are 2.340(15) and 2.350(13) Å, which are significantly shorter than those of 2.386(13) and 2.416(14) Å for Hg1−N distances, which may

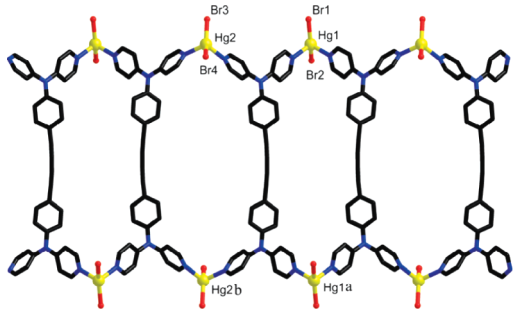

Figure 5. Ladder-like structure approximately along the *c* axis in the crystal of complex **5**. Symmetry operations: (a) $-x - 1/2, -y + 1/2, -z + 1$; (b) $-x + 1/2, -y + 1/2, -z + 1$.

also be caused by the presence of the embowed conformation. Thus, two different 46-membered metallomacrocycles are formed with the distances of 22.78 Å and 21.59 Å for Hg1···Hg1a and Hg2···Hg2b, respectively. Finally, these metallomacrocycles are linked to afford a ladder-like structure approximately along the *c* axis.

Crystal structure of $[Cu_2LI_2]_n \cdot 0.5n CH_2Cl_2$ (6). The structure of complex **6** is shown in Figure 6. The coordination

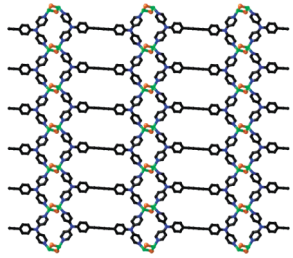

Figure 6. 2D network of **6** with two different metallomacrocycles.

sphere around each Cu(I) center is composed of two pyridyl N atoms and two iodine anions, with Cu−N bond lengths of 2.040(7) and 2.066(7) Å, and Cu−I bond lengths of 2.714(2) and 2.627(2) Å. These bond lengths are comparable to those observed in similar complexes.[20]

Two neighboring Cu(I) atoms are bridged by two iodides with the Cu(I)−I−Cu(I) bridging angles of 120.61(5)°, thus affording Cu_2I_2 units, which are further linked by the tetrapyridyl L ligands to form a 2D coordination network composed of 46- and 24-membered metallomacrocycles. Cu_2I_2 units can be simplified as four-connected cluster nodes, thus the topology of **6** is a uninodal 4^4-**sql** net, which is similar to that of complex **3**.

Crystal Structure of $[Ag_2L(H_2O)_2]_n(NO_3)_{2n} \cdot 2nH_2O$ (7). The crystallographic asymmetric unit of complex **7** (Figure 7) comprises a $[Ag_2L]^{2+}$ cation, two weakly coordinated water

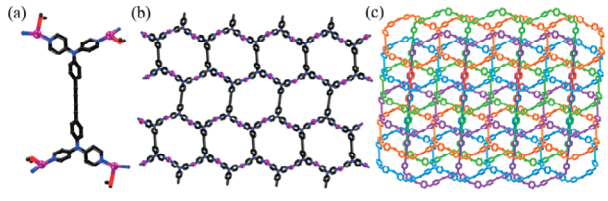

Figure 7. (a) Coordination mode of ligand L in complex **7**. (b) An undulated 2D network with large cavities (c) A 4-fold interpenetrated 2D structure of **7**.

dx.doi.org/10.1021/cg201655n | *Cryst. Growth Des.* 2012, 12, 3465−3473

molecules and two noncoordinated nitrate anions. Each Ag(I) atom is coordinated to two N atoms from two L ligands with the Ag−N bond lengths of 2.156(6) and 2.139(7) Å, and N−Ag−N bond angle of 159.3(3)°. Distortion of the N−Ag−N moiety from an ideal line is related to the weak coordination of a water molecule with the Ag−O bond length of 2.684(1) Å. The final coordination geometry around Ag(I) is approximately T-shaped with O−Ag−N angles of 103.4(4) and 96.7(4)°. Thus, each L ligand links four Ag(I) ions and each Ag(I) ion links two L ligands, resulting in the formation of undulated with large cavities composed of 66-membered metallomacrocycles. Topologically, the central N atoms of dpa units can be considered as three-connected nodes and the 2D sheet can be described as a typical 6^3-**hcb** net, which is interpenetrated by three other such 6^3-**hcb** nets, affording a 4-fold interpenetrated structure.

Photoluminescence. Coordination polymers with d^{10} metal centers and conjugated organic linkers have potential applications in various areas such as luminescent materials and chemical sensors.[21] Hence, the solid state photoluminescence properties of complexes **1**−**7**, together with the crystalline samples of the free ligand L and L·0.5DMF were investigated at room temperature (Figure 8). The free ligand L exhibits a

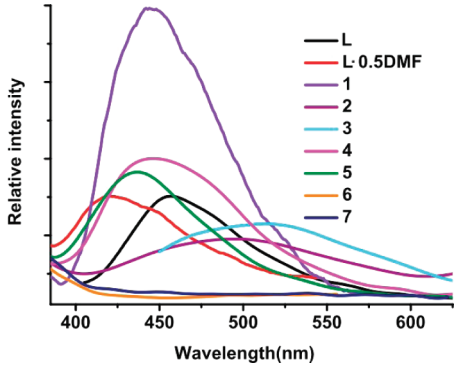

Figure 8. Emission spectra of L, L·0.5DMF, and compounds **1**−**7** in the solid state at room temperature.

medium-intensity emission centered at 457 nm upon excitation at 330 nm, which may be attributed to the $\pi^* \rightarrow \pi$ transition.[22] In contrast, the main peak for L·0.5DMF is blue-shifted to a λ_{max} of 420 nm, which may result from a decrease in the π conjugation system caused by the bent conformation observed its crystal structure (vide supra).

For complex **1**, intense emission band is observed at 444 nm, upon excitation at 310 nm, which is blue-shifted as compared to that of L. Considering the bent conformation of the ligand in this complex, it is more reasonable to compare it with L·0.5 DMF, which has a similar bent conformation. Thus, the emission at 444 nm is red-shifted compared to that of 420 nm for L·0.5 DMF. This result is consistent with previous observations.[7a] Complexes **2** and **3** in the solid state have very broad emission bands with λ_{max} values of 496 and 515 nm, respectively, which are red-shifted, as compared with the corresponding values of the ligand crystals. Because the Cd(II) ions are difficult to oxidize or to reduce, the emissions of **2** and **3** are neither metal-to-ligand charge transfer (MLCT) nor ligand-to-metal charge transfer (LMCT) in nature.[23]

As a result, the emissions may be tentatively attributed to the intraligand transitions.[24] It is clear that a further red shift of the emission occurs for **3**, compared with complex **2**, which is probably due to the differences of anions and coordination environment around the central metal ions, because photoluminescent behavior is closely associated with the local environments around metal ions.[25] Furthermore, the bent conformation of the ligands observed in complex **2** may also cause a blue shift of the emission band due to the decrease of the π conjugation system. Therefore, the emission at a longer wavelength is observed for **3**, as compared to that of **2**. The emissions of complexes **2** and **3** are significantly weaker than that of L, which may be ascribed to the heavy-atom effect.[26] Obviously, the emission bands of **4** centered 442 nm also can be attributed to the intraligand transitions because of its similarity with that of L.[24c,27]

It is noteworthy that the intensity for **4** is stronger than that of the ligand, which may be related to the suppression of nonemissive energy-loss mechanism, probably induced by the better rigidity imparted by the tethering of the $\{Cd_6(SO_4)_6\}_\infty$ chain motifs. Complex **5** in the solid state exhibits a slightly blue-shifted emission band (λ_{max} = 437 nm) with respect to the free L ligand. This observation is similar to that for complex **1**, and it also may be related to the bent conformation of the ligands, similar to that observed in complex **1**. In contrast to these compounds, no clear luminescence was detected for **6** and **7**, which may be related to the heavy atom effect.

Compared to our previously reported ligand L^2 (Scheme 1) and its corresponding complexes, the emission peaks of L and its complexes **2**, **3**, **5** exhibit red shifts of 46, 61, 44, and 23 nm, respectively. This observation is consistent with our expectation of increasing the emission wavelength by extending the π conjugation system through the introduction of a butadiyne unit, and it is consistent with the calculated values of HOMO−LUMO energy gaps of 4.44 and 3.45 ev for L^2 and L, respectively (Supporting Information Table S3 and Figure S5).

■ CONCLUSIONS

One novel tetrapyridyl ligand bis(4,4′-dipyridylamino-phenylene)butadiyne (L) containing a butadiyne unit was prepared and used to coordinate with d^{10} metals, including Zn(II), Cd(II), Hg(II), Cu(I) and Ag(I) to afford a rich variety of complexes. The crystals of **1** and **5** exhibit ladder-like structures with the embowed-conformation ligands. **2** exhibits a 2-fold interpenetrated 3D network, and **4** exhibits a 3D coordination network consisting of infinite $\{Cd_6(SO_4)_6\}_\infty$ chains. Complexes **3**, **6**, and **7** exhibit 2D structures, in which **3** consists of 46- and 20-membered metallomacrocycles, **6** is composed of 46- and 24-membered metallomacrocycles, and **7** exhibit 4-fold interpenetrated 2D sheets with the cavities composed of 66-membered metallomacrocycles. The photoluminescence measurements illustrated that L, L·0.5DMF and complexes **1**−**7** exhibited emissions with the maxima wavelengths varying in a large range of 420−515 nm. The variation in emission intensities and wavelengths can be rationalized in terms of the metal centers, the anions, the extended aromatic systems and the flexible butadiyne units. The conformational flexibility of the butadiyne moiety was observed, which provides additional means for modulating the structures and luminescent properties. Furthermore, it can be expected that design and utilization of similar tetrapyridyl ligands with the butadiyne unit connected to the pyridine rings in stead of the N atom is a practical approach of further extending the aromatic systems to further tune the fluorescence wavelength and intensity, which is underway in our lab.

dx.doi.org/10.1021/cg201655n | *Cryst. Growth Des.* 2012, 12, 3465−3473

■ ASSOCIATED CONTENT

Supporting Information

Crystallographic information files (CIF format), the crystal information of complex **1**, the calculated HOMO/LUMO energies of L^2 and L, NMR spectra and HRMS of L, and part of the crystal figures. This material is available free of charge via the Internet at http://pubs.acs.org.

■ AUTHOR INFORMATION

Corresponding Author

*E-mail: yshxie@ecust.edu.cn.

Notes

The authors declare no competing financial interest.

■ ACKNOWLEDGMENTS

This work was financially supported by NSFC (21072060), the Program for Professor of Special Appointment (Eastern Scholar) at Shanghai Institutions of Higher Learning, Program for New Century Excellent Talents in University (NCET), Innovation Program of Shanghai Municipal Education Commission, the Fundamental Research Funds for the Central Universities (WK1013002), and SRFDP (20100074110015). S.W. Ng is grateful for support by the University of Malaya (UM.C/625/1/HIR/033/10).

■ REFERENCES

(1) (a) Ni, Z. H.; Kou, H. Z.; Zhang, L. F.; Ge, C.; Cui, A. L.; Wang, R. J.; Li, Y.; Sato, O. *Angew. Chem., Int. Ed.* **2005**, *44*, 7742. (b) Kaye, S. S.; Dailly, A.; Yaghi, O. M.; Long, J. R. *J. Am. Chem. Soc.* **2007**, *129*, 14176. (c) Hembury, G. A.; Borovkov, V. V.; Inoue, Y. *Chem. Rev.* **2008**, *108*, 15a. (d) Li, C. J.; Lin, Z. J.; Peng, M. X.; Leng, J. D.; Yang, M. M.; Tong, M. L. *Chem. Commun.* **2008**, 6348. (e) Wu, M. Y.; Jiang, F. L.; Wei, W.; Gao, Q.; Huang, Y. G.; Chen, L.; Hong, M. C. *Cryst. Growth Des.* **2009**, *9*, 2559. (f) Zhang, Y. B.; Zhang, W. X.; Feng, F. Y.; Zhang, J. P.; Chen, X. M. *Angew. Chem., Int. Ed.* **2009**, *48*, 5287. (g) Zheng, B. S.; Bai, J. F.; Duan, J. G.; Wojtas, L.; Zaworotko, M. J. *J. Am. Chem. Soc.* **2010**, *133*, 748. (h) Qiu, W. G.; Perman, J. A.; Wojtas, L.; Eddaoudi, M.; Zaworotko, M. J. *Chem. Commun.* **2010**, *46*, 8734. (i) Han, D.; Jiang, F. L.; Wu, M. Y.; Chen, L.; Chen, Q. H.; Hong, M. C. *Chem. Commun.* **2011**, *47*, 9861.

(2) (a) Lan, A. J.; Li, K. H.; Wu, H. H.; Olson, D. H.; Emge, T. J.; Ki, W.; Hong, M. C.; Li, J. *Angew. Chem., Int, Ed.* **2009**, *48*, 2334. (b) Liu, Y.; Xu, X.; Xia, Q. C.; Yuan, G. Z.; He, Q. Z.; Cui, Y. *Chem. Commun.* **2010**, *46*, 2608. (c) Liu, J. L.; Bao, X.; Leng, J. D.; Lin, Z. J.; Tong, M. L. *Cryst. Growth Des.* **2011**, *11*, 2398. (d) Albiol, D. F.; O'Brien, T. A.; Wernsdorfer, W.; Moulton, B.; Zaworotko, M. J.; Abboud, K. A.; Christou, G. *Angew. Chem., Int. Ed.* **2005**, *44*, 897. (e) Mishra, A.; Tasiopoulos, A. J.; Wernsdorfer, W.; Moushi, E. E.; Moulton, B.; Zaworotko, M. J.; Abboud, A. K.; Christou, G. *Inorg. Chem.* **2008**, *47*, 4832.

(3) (a) Hu, T. L.; Zou, R. Q.; Li, J. R.; Bu, X. H. *Dalton Trans.* **2008**, 1302. (b) Chen, W.; Wang, J. Y.; Chen, C.; Yue, Q.; Yuan, H. M.; Chen, J. S.; Wang, S. N. *Inorg. Chem.* **2003**, *42*, 944. (c) Cui, P.; Chen, Z.; Gao, D. L.; Zhao, B.; Shi, W.; Cheng, P. *Cryst. Growth Des.* **2010**, *10*, 4370. (d) Sun, Y. Q.; Zhang, J.; Chen, Y. M.; Yang, G. Y. *Angew. Chem., Int. Ed.* **2005**, *44*, 5814.

(4) (a) Das, S.; Bhar, K.; Chantrapromma, S.; Fun, H. K.; Kanaparthi, R. K.; Samanta, A.; Ghosh, B. K. *Inorg. Chim. Acta* **2011**, *367*, 199. (b) Park, B. K.; Eom, G. H.; Kim, S. H.; Kwak, H.; Yoo, S. M.; Lee, Y. J.; Kim, C.; Kim, S. J.; Kim, Y. *Polyhedron* **2010**, *29*, 773. (c) Wang, X. T.; Wang, X. H.; Wang, Z. M.; Gao, S. *Inorg. Chem.* **2009**, *48*, 1301. (d) Baca, S. G.; Malaestean, I. L.; Keene, T. D.; Adams, H.; Ward, M. D.; Hauser, J.; Neels, A.; Decurtins, S. *Inorg. Chem.* **2008**, *47*, 1110811. (e) Lee, Y. M.; Hong, S. J.; Kim, H. J.; Lee, S. H.; Kwak, H.; Kim, C.; Kim, S. J.; Kim, Y. *Inorg. Chem. Commun.* **2007**, *10*, 287. (f) Jia, W. L.; Wang, R. Y.; Song, D. T.; Ball, S. J.; McLean, A. B.; Wang, S. N. *Chem.—Eur. J.* **2005**, *11*, 832.

(5) (a) Sposato, L. K.; Nettleman, J. H.; Braverman, M. A.; Supkowski, R. M.; LaDuca, R. L. *Cryst. Growth Des.* **2010**, *10*, 335. (b) Farnum, G. A.; Nettleman, J. H.; LaDuca, R. L. *CrystEngComm* **2010**, *12*, 888. (c) Shyu, E.; Supkowski, R. M.; LaDuca, R. L. *Cryst. Growth Des.* **2009**, *9*, 2481. (d) Martin, D. P.; Montney, M. R.; Supkowski, R. M.; LaDuca, R. L. *Cryst. Growth Des.* **2008**, *8*, 3091. (e) Hao, Z. M.; Zhang, X. M. *Cryst. Growth Des.* **2007**, *7*, 64.

(6) (a) Ross, T. M.; Moubaraki, B.; Turner, D. R.; Halder, G. J.; Chastanet, G.; Neville, S. M.; Cashion, J. D.; Letard, J. F.; Batten, S. R.; Murray, K. S. *Eur. J. Inorg. Chem.* **2011**, 1395. (b) Sumby, C. J. *Coord. Chem. Rev.* **2011**, *255*, 1937. (c) Kuo, J. H.; Tsao, T. B.; Lee, G. H.; Lee, H. W.; Yeh, C. Y.; Peng, S. M. *Eur. J. Inorg. Chem.* **2011**, 2025.

(7) (a) Zeng, F. H.; Ni, J.; Wang, Q. G.; Ding, Y. B.; Ng, S. W.; Zhu, W. H.; Xie, Y. S. *Cryst. Growth Des.* **2010**, *10*, 1611. (b) Wei, K. J.; Xie, Y. S.; Ni, J.; Zhang, M.; Liu, Q. L. *Cryst. Growth Des.* **2006**, *6*, 1341. (c) Wang, Q. G.; Xie, Y. S.; Zeng, F. H.; Ng, S. W.; Zhu, W. H. *Inorg. Chem. Commun.* **2010**, *13*, 929. (d) Wei, K. J.; Ni, J.; Xie, Y. S.; Liu, Q. L. *Inorg. Chem. Commun.* **2007**, *10*, 279. (e) Wei, K. J.; Xie, Y. S.; Ni, J.; Zhang, M.; Liu, Q. L. *Inorg. Chem. Commun.* **2006**, *9*, 926.

(8) Karnbratt, J.; Hammarson, M.; Li, S. M.; Anderson, H. L.; Albinsson, B.; Andreasson, J. *Angew. Chem., Int. Ed.* **2010**, *49*, 1854.

(9) Sheldrick, G. M. *Acta Crystallogr. A* **2008**, *64*, 112.

(10) Frisch, M. J.; Trucks, G. W.; Schlegel, H. B.; Scuseria, G. E.; Robb, M. A.; Cheeseman, J. R.; Montgomery, Jr., J. A.; Vreven, T.; Kudin, K. N.; Burant, J. C.; Millam, J. M.; Iyengar, S. S.; Tomasi, J.; Barone, V.; Mennucci, B.; Cossi, M.; Scalmani, G.; Rega, N., Petersson, G. A.; Nakatsuji, H.; Hada, M.; Ehara, M.; Toyota, K.; Fukuda, R.; Hasegawa, J.; Ishida, M.; Nakajima, T.; Honda, Y.; Kitao, O.; Nakai, H.; Klene, M.; Li, X.; Knox, J. E.; Hratchian, H. P.; Cross, J. B.; Bakken, V.; Adamo, C.; Jaramillo, J.; Gomperts, R.; Stratmann, R. E.; Yazyev, O.; Austin, A. J.; Cammi, R.; Pomelli, C.; Ochterski, J. W.; Ayala, P. Y.; Morokuma, K.; Voth, G. A.; Salvador, P.; Dannenberg, J. J.; Zakrzewski, V. G.; Dapprich, S.; Daniels, A. D.; Strain, M. C.; Farkas, O.; Malick, D. K.; Rabuck, A. D.; Raghavachari, K.; Foresman, J. B.; Ortiz, J. V.; Cui, Q.; Baboul, A. G.; Clifford, S.; Cioslowski, J.; Stefanov, B. B.; Liu, G.; Liashenko, A.; Piskorz, P.; Komaromi, I.; Martin, R. L.; Fox, D. J.; Keith, T.; Al-Laham, M. A.; Peng, C. Y.; Nanayakkara, A.; Challacombe, M.; Gill, P. M. W.; Johnson, B.; Chen, W.; Wong, M. W.; Gonzalez, C. Pople, J. A. *Gaussian 03*, revision C.02; Gaussian, Inc.: Wallingford, CT, 2004.

(11) (a) Becke, A. D. *J. Chem. Phys.* **1993**, *98*, 5648. (b) Lee, C.; Yang, W.; Parr, R. G. *Phys. Rev. B* **1988**, *37*, 785.

(12) (a) Hay, P. J.; Wadt, W. R. *J. Chem. Phys.* **1985**, *82*, 270. (b) Wadt, W. R.; Hay, P. J. *J. Chem. Phys.* **1985**, *82*, 284. (c) Hay, P. J.; Wadt, W. R. *J. Chem. Phys.* **1985**, *82*, 299.

(13) Allouche, A. R. *J. Comput. Chem.* **2011**, *32*, 174.

(14) (a) Nishihara, Y.; Ikegashira, K.; Hirabayashi, K.; Ando, J.; Mori, A.; Hiyama, T. *J. Org. Chem.* **2000**, *65*, 1780. (b) Yue, W.; Zhen, Y. G.; Li, Y.; Jiang, W.; Lv, A. F.; Wang, Z. H. *Org. Lett.* **2010**, *12*, 3460.

(15) (a) Tsuzuki, S.; Honda, K.; Uchimaru, T.; Mikami, M.; Tanabe, K. *J. Am. Chem. Soc.* **2002**, *124*, 104. (b) Kamishima, M.; Kojima, M.; Yoshikawa, Y. *J. Comput. Chem.* **2001**, *22*, 835. (c) Janiak, C. *J. Chem. Soc., Dalton Trans.* **2000**, 3885.

(16) (a) Hu, S.; Meng, Z. S.; Tong, M. L. *Cryst. Growth Des.* **2010**, *10*, 1742. (b) Turner, D. R.; Smith, B.; Goeta, A. E.; Evans, I. R.; Tocher, D. A.; Howard, J. A. K.; Steed, J. W. *CrystEngComm* **2004**, *6*, 633.

(17) (a) Blatov, V. A. *IUCr CompComm. Newsletter* **2006**, *7*, 4. (b) Blatov, V. A.; Shevchenko, A. P.; Serezhkin, V. N. *J. Appl. Crystallogr.* **2000**, *33*, 1193.

(18) (a) Lee, T. G.; Lee, J. H.; Hyun, M. Y.; Jang, S. P.; Lee, H. G.; Kim, C.; Kim, S. J.; Kim, Y. *Inorg. Chem. Commun.* **2010**, *13*, 1493. (b) Bai, H. Y.; Ma, J. F.; Yang, J.; Liu, Y. Y.; Hua, W.; Ma, J. C. *Cryst. Growth Des.* **2009**, *10*, 995. (c) Tzeng, B. C.; Lu, Y. M.; Lee, G. H.; Peng, S. M. *Eur. J. Inorg. Chem.* **2006**, *2006*, 1698.

(19) (a) Paul, A. K.; Sanyal, U.; Natarajan, S. *Cryst. Growth Des.* **2010**, *10*, 4161. (b) Li, G. J.; Xing, Y.; Song, S. Y.; Xu, N.; Liu, X. C.; Su, Z.

M. *J. Solid State Chem.* **2008**, *181*, 2406. (c) Liu, D. S.; Huang, G. S.; Huang, C. C.; Huang, X. H.; Chen, J. Z.; You, X. Z. *Cryst. Growth Des.* **2009**, *9*, 5117. (d) Papatriantafyllopoulou, C.; Kostakis, G. E.; Raptopoulou, C. P.; Terzis, A.; Perlepes, S. P.; Plakatouras, J. C. *Inorg. Chim. Acta* **2009**, *362*, 2361.

(20) (a) Deng, Z. P.; Qi, H. L.; Huo, L. H.; Ng, S. W.; Zhao, H.; Gao, S. *Dalton Trans.* **2010**, *39*, 10038. (b) Kang, E. J.; Lee, S. Y.; Lee, H.; Lee, S. S. *Inorg. Chem.* **2010**, *49*, 7510.

(21) (a) Yue, C. Y.; Yan, C. F.; Feng, R.; Wu, M. Y.; Chen, L.; Jiang, F. L; Hong., M. C. *Inorg. Chem.* **2009**, *48*, 2873. (b) Allendorf, M. D.; Bauer, C. A.; Bhaktaa, R. K.; Houka, R. J. T. *Chem. Soc. Rev.* **2009**, *38*, 1330. (c) Hu, J.; Zhao, J.; Guo, Q.; Hou, H.; Fan, Y. *Inorg. Chem.* **2010**, *49*, 3679. (d) Yao, X. Q.; Cao, D. P.; Hu, J. S.; Li, Y. Z.; Guo, Z. J.; Zheng, H. G. *Cryst. Growth Des.* **2011**, *11*, 231. (e) Li, L.; Luo, J. H.; Wang, S. Y.; Sun, Z. H.; Chen, T. L.; Hong, M. C. *Cryst. Growth Des.* **2011**, *11*, 3744.

(22) (a) Shi, X.; Zhu, G. S.; Fang, Q. R.; Wu, G.; Tian, G.; Wang, R. W.; Zhang, D. L.; Xue, M.; Qiu, S. L. *Eur. J. Inorg. Chem.* **2004**, 185. (b) Zhang, X. M.; Tong, M. L.; Gong, M. L.; Chen, X. M. *Eur. J. Inorg. Chem.* **2003**, 138. (c) Tian, G.; Zhu, G. S.; Fang, Q. R.; Guo, X. D.; Xue, M.; Sun, J. Y.; Qiu, S. L. *J. Mol. Struct.* **2006**, *787*, 45.

(23) (a) Wen, L. L.; Li, Y. Z.; Lu, Z. D.; Lin, J. G.; Duan, C. Y.; Meng, Q. J. *Cryst. Growth Des.* **2006**, *6*, 530. (b) Wen, L. L.; Lu, Z. D.; Lin, J. G.; Tian, Z. F.; Zhu, H. Z.; Meng, Q. J. *Cryst. Growth Des.* **2007**, *7*, 93. (c) Lin, J. G.; Zang, S. Q.; Tian, Z. F.; Li, Y. Z.; Xu, Y. Y.; Zhu, H. Z.; Meng, Q. J. *CrystEngComm* **2007**, *9*, 915.

(24) (a) Jia, W. W.; Luo, J. H.; Zhu, M. L. *Cryst. Growth Des.* **2011**, *11*, 2386. (b) Chen, L. J.; He, X.; Xia, C. K.; Zhang, Q. Z.; Chen, J. T.; Yang, W. B.; Lu, C. Z. *Cryst. Growth Des.* **2006**, *6*, 2076. (c) Dong, B. X.; Xu, Q. *Cryst. Growth Des.* **2009**, *9*, 2776. (d) Zhang, R. B.; Li, Z. J.; Cheng, J. K.; Qin, Y. Y.; Zhang, J.; Yao, Y. G. *Cryst. Growth Des.* **2008**, *8*, 2562.

(25) (a) Fu, Z. Y.; Wu, X. T.; Dai, J. C.; Hu, S. M.; Du, W. X.; Zhang, H. H.; Sun, R. Q.; Eur., J. *Inorg. Chem.* **2002**, 2730. (b) Wen, L. L.; Dang, D. B.; Duan, C. Y.; Li, Y. Z.; Tian, Z. F.; Meng, Q. J. *Inorg. Chem.* **2005**, *44*, 7161. (c) Zhang, Y. N.; Liu, P.; Wang, Y. Y.; Wu, L. Y.; Pang, L. Y.; Shi, Q. Z. *Cryst. Growth Des.* **2011**, *11*, 1531.

(26) (a) Drago, R. S. *Physical Methods in Chemistry*; Saunders: Philadelphia, PA, 1977; Chapter 5. (b) Masetti, F.; Mazzucato, U.; Galiazzo, G *J. Lumin.* **1971**, *4*, 8. (c) Warner, T. C.; Hawkins, W.; Facci, J.; Torrisi, R.; Trembath, T. *J. Phys. Chem.* **1978**, *82*, 298. (d) Aragoni, M. C.; Arca, M.; Demartin, F.; Devillanova, F. A.; Isaia, F.; Garau, A.; Lippolis, V.; Jalali, F.; Papke, U.; Shamsipur, M.; Tei, L.; Yari, A.; Verani, G. *Inorg. Chem.* **2002**, *41*, 6623. (e) Seward, C.; Chan, J.; Song, D.; Wang, S. N. *Inorg. Chem.* **2003**, *42*, 1112.

(27) Xu, C.; Guo, Q.; Wang, X.; Hou, H.; Fan, Y. *Cryst. Growth Des.* **2011**, *11*, 1869.